The asymptotic structure of a shear band in mode-II deformations

L. Chen, R.C. Batra*

Department of Engineering Science and Mechanics, Mail Code 0219, Virginia Polytechnic Institute and State University, Blacksburg, VA 24061, USA

Abstract

A shear band is assumed to propagate at a uniform velocity in a thermoviscoplastic body being deformed in mode-II. The deformation field appears steady to an observer situated on and moving with the shear band tip. The region around the shear band tip is divided into a core region and an inertial region. The core region is behind the shear band tip, and the inertial region surrounds the band tip but excludes a small region around the tip. Asymptotic fields for the velocity, temperature and the effective stress are determined in the inertial region. The dependencies of the thermal width of the band and of the rate of energy dissipated within the core region behind the shear band-tip upon the speed of the shear band are exhibited. © 1999 Elsevier Science Ltd. All rights reserved.

1. Introduction

Tresca [1] and Massey [2] observed shear bands during the hot forging of a platinum bar. Subsequently, Zener and Hollomon [3] reported 20 μm wide shear bands during the punching of a hole in a low carbon steel plate, and postulated that a material point becomes unstable when its hardening due to strain and strain-rate effects is overcome by the softening due to its being heated up. Experimental work [4] on torsional tests of thin-walled tubes has revealed that a shear band initiates much later than when a material point becomes unstable. Batra and Kim [5] and Deltort [6] have postulated that a shear band initiates in earnest at a material point when the shear stress there has dropped to 90 and 80%, respectively, of its peak value. Much

---

* Corresponding author. Tel.: + 1 540 231 6051; fax: + 1 540 231 4574.
  E-mail address: rbatra@vt.edu (R.C. Batra)

of the work on adiabatic shear bands is summarized in the book by Bai and Dodd [7], the review paper by Tomita [8], in papers included in the special issue of the *Applied Mechanics Reviews* [9], and the *Mechanics of Materials* journal [10], and in lecture notes [11] edited by Perzyna.

In a torsion test on a homogeneous and isotropic thick-walled tube with a *V*-notch around its circumference, a shear band propagates in a direction normal to the particle velocity [12]. If a shear band were to be replaced by a crack, this will correspond to mode III deformations. Kalthoff [13], Mason et al. [14] and Zhou et al. [15] have experimentally studied the initiation and propagation of a shear band in a prenotched plate impacted on the notched side by a projectile moving parallel to the axis of the notch. The deformation field near the notch tip is dominated by mode II deformations. Needleman and Tvergaard [16], Zhou et al. [17] and Batra and Nechitailo [18] have analysed this problem numerically under the assumption of the plane strain state of deformation.

Wright and Walter [19] have studied the asymptotic structure of a shear band propagating at a uniform velocity in a rigid thermoviscoplastic material being deformed in antiplane shear. They divided the region around the shear band tip into a core region that is behind the shear band tip and an inertial region surrounding the shear band tip but excluding an infinitesimal region around it. Whereas both heat conduction and inertia forces are dominant in the core region, only inertia forces are considered in the inertial region. In antiplane shear, there is only one component of velocity directed normal to the plane of deformation. Here we extend their work to a rigid thermoviscoplastic body being deformed in mode II or in-plane shearing. It is found that with an increase in the shear band speed, the thermal width of the band sharply decreases but the rate of energy dissipated per unit volume of the core region behind the band tip rapidly increases.

2. Formulation of the problem

We study thermomechanical deformations near the tip of a shear band which is propagating horizontally at a constant speed U in a thermoviscoplastic body undergoing mode II deformations. The deformations are assumed to be steady with respect to an observer situated on and moving with the shear band tip. Consider a cylindrical coordinate system with origin at the position of the shear band tip at time $t = 0$ as shown in Fig. 1. We neglect elastic deformations and assume the material to be incompressible; the material is thus modeled as rigid thermoviscoplastic. This is justified because within and adjacent to the shear band, plastic deformations are very large. Equations governing the thermomechanical deformations of the body are

$$\text{tr}\mathbf{D} = 0, \tag{1}$$

$$\rho\dot{\mathbf{v}} = \text{div}\mathbf{S} - \nabla p, \tag{2}$$

$$\rho c_{\text{v}}\dot{T} = k\nabla^2 T + \text{tr}(\mathbf{SD}), \tag{3}$$
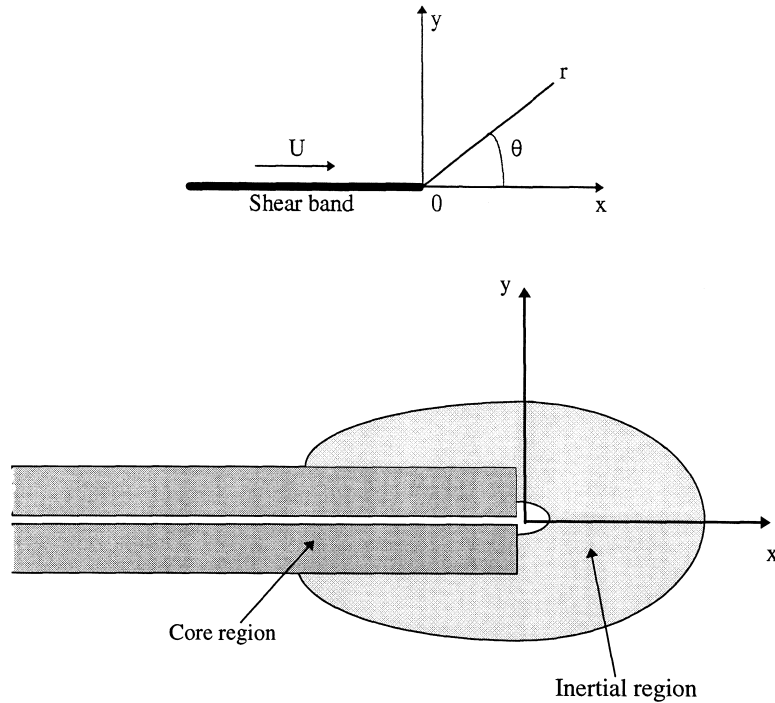
Fig. 1. A schematic sketch of the problem studied, and illustrations of the core and inertial regions.

$$\mathbf{S} = 2k_0(1 - \alpha T)(1 + bI)^m \mathbf{D}/I. \tag{4}$$

Eqs. (1)–(4) express, respectively, the balance of mass, balance of linear momentum, balance of internal energy and the constitutive relation for a thermoviscoplastic body. In them, $\mathbf{D}$ is the strain-rate tensor, ρ the mass density, $\mathbf{v}$ the velocity field, $\mathbf{S}$ the deviatoric Cauchy stress tensor, p the hydrostatic pressure, c_v the specific heat, k the thermal conductivity, T the temperature rise, k_0 a strength parameter, α the thermal softening coefficient, $I^2 \equiv (2\text{tr } \mathbf{D}^2)$ an invariant of the strain-rate tensor, b the rate constant and m the strain-rate sensitivity parameter. A superimposed dot indicates the material time derivative and operators div and tr signify the divergence and trace operators. The body force and the source of internal energy have been neglected. Also, Fourier's law of heat conduction has been assumed, and both the specific heat and the thermal conductivity are taken to be constants. The constitutive relation (4) is a generalization, due to Batra [20], of the one-dimensional relation proposed by Litonski [21] to three-dimensional problems. Batra [20] and others [22,23] have used it to analyse steady state penetration problems. It has also been employed by Batra and Liu [24] and Wright and Walter [19] to study shear bands in thermoviscoplastic materials.

We nondimensionalize variables in a way similar to that done by Wright and Batra [25]. That is, we scale distance with the half-width H of the slab, time with the reciprocal of the nominal strain-rate $\dot{\gamma}_0$, stress with k_0, and temperature with $k_0/(\rho c_v)$. For a typical hard steel, $\rho = 8000$ kg/m^3, $c_v = 448$ J/(Kg K), $k_0 = 330$ MPa, $b = 10^4$ s, $\alpha = 0.0008$/K, $k = 50$ W/(mK). In terms of non-dimensional variables, Eqs. (1)–(4) look as before except that $k_0 = 1$ in Eq.

(4), and the coefficient of $\dot{T}$ in Eq. (3) equals 1. At a nominal strain-rate $\dot{\gamma}_0$ of 10^5/s and $H = 2.5$ mm, the coefficient of $\dot{\mathbf{v}}$ in Eq. (2) equals nearly 1.0, and that of $\nabla^2 T$ in Eq. (3) 2.23×10^{-5}. Hence, there will be a thermal boundary layer formed adjacent to the hot shear-banded region. Following Wright and Walter [19], we call the small region behind the shear band tip the core region. Heat conduction is neglected in regions far away from the shear band; however, inertial effects are considered. The core and inertial regions are sketched in Fig. 1.

2.1. Inertial solution

The balance of mass or the continuity Eq. (1) is identically satisfied by expressing the radial and tangential components u, v of the velocity $\mathbf{v}$ in terms of a stream function ϕ.

$$u = \frac{1}{r}\frac{\partial \phi}{\partial \theta} = \frac{1}{r}\phi_{,\theta}, \quad v = -\frac{\partial \phi}{\partial r} = -\phi_{,r}. \tag{5}$$

Substitution from Eq. (5) into Eqs. (2)–(4) yields

$$\frac{2}{r}\frac{\partial}{\partial r}\left(r\frac{s}{I}D_{rr}\right) + \frac{2}{r}\frac{\partial}{\partial \theta}\left(\frac{s}{I}D_{r\theta}\right) + \frac{2}{r}\frac{s}{I}D_{rr} - \frac{\partial p}{\partial r} = \rho\dot{u}, \tag{6}$$

$$\frac{2}{r}\frac{\partial}{\partial r}\left(r\frac{s}{I}D_{r\theta}\right) - \frac{2}{r}\frac{\partial}{\partial \theta}\left(\frac{s}{I}D_{rr}\right) + \frac{2}{r}\frac{s}{I}D_{r\theta} - \frac{1}{r}\frac{\partial p}{\partial \theta} = \rho\dot{v}, \tag{7}$$

$$k\left[\frac{1}{r}\frac{\partial}{\partial r}(rg_{,r}) + \frac{1}{r^2}g_{,\theta\theta}\right] - \alpha s I = \rho c_{\mathrm{v}}\dot{g}, \tag{8}$$

$$I = 2(D_{rr}^2 + D_{r\theta}^2)^{1/2}, \tag{9}$$

$$s = k_0 g(1 + bI)^m, \tag{10}$$

$$g = 1 - \alpha T, \tag{11}$$

where

$$D_{rr} = \frac{1}{r}\phi_{,r\theta} - \frac{1}{r^2}\phi_{,\theta}, \tag{12}$$

$$D_{r\theta} = \frac{1}{2}\left(\frac{1}{r^2}\phi_{,\theta\theta} + \frac{1}{r}\phi_{,r} - \phi_{,rr}\right), \tag{13}$$

are deviatoric strain-rates, and $s = (\mathrm{tr}\ SS^{\mathrm{T}})^{1/2}/2$. The non-zero components of the Cauchy stress tensor, $\boldsymbol{\sigma} = -p\mathbf{1} + \mathbf{S}$, are given by

$$\sigma_{rr} = 2\frac{s}{I}D_{rr} - p, \tag{14}$$

$$\sigma_{\theta\theta} = -2\frac{s}{I}D_{rr} - p, \tag{15}$$

$$\sigma_{r\theta} = 2\frac{s}{I}D_{r\theta}. \tag{16}$$

The elimination of pressure p from Eqs. (6) and (7) gives

$$\frac{2}{r}\left(r\frac{s}{I}D_{rr}\right)_{,r\theta} + 2\left(\frac{s}{I}D_{rr}\right)_{,r\theta} + \frac{2}{r}\left(\frac{s}{I}D_{r\theta}\right)_{,\theta\theta} - 2\left(r\frac{s}{I}D_{r\theta}\right)_{,rr} + 2\left(\frac{1}{r}\frac{s}{I}D_{rr}\right)_{,\theta} - 2\left(\frac{s}{I}D_{r\theta}\right)_{,r}$$

$$= \rho(\dot{u}_{,\theta} - \dot{v} - r\dot{v}_{,r}). \tag{17}$$

In order to develop an asymptotic solution, we introduce below a new polar coordinate system $\bar{r}$, ψ centered at and moving with the shear band tip in the r, θ plane. Thus

$$\bar{r} = [(r\cos\theta - Ut)^2 + (r\sin\theta)^2]^{1/2}, \tag{18}$$

$$\psi = \tan^{-1}\left(\frac{r\sin\theta}{r\cos\theta - Ut}\right). \tag{19}$$

As the shear band tip moves into the relatively undeformed material, we presume that deformation fields appear steady to an observer situated on and moving with the shear band tip. Thus ϕ and other field variables depend only upon $\bar{r}$ and ψ and not explicitly on time t. Since the coordinate system $\bar{r}$, ψ moves with a uniform velocity U in the horizontal direction, it constitutes an inertial frame of reference. Eqs. (5) and (8)–(17), when written in the $\bar{r}$, ψ coordinate system, look as before with the velocity components taken along the translating axes except that r and θ are replaced by $\bar{r}$ and ψ, respectively,

$$\dot{u} = (u - U)\left(\cos\psi\, u_{,\bar{r}} - \frac{\sin\psi}{\bar{r}}\bar{u}_{,\psi}\right) + v\left(\sin\psi\, u_{,\bar{r}} + \frac{\cos\psi}{\bar{r}}u_{,\psi}\right), \tag{20}$$

and similar expressions hold for $\dot{v}$ and $\dot{g}$. Henceforth, we omit the superimposed bar on r.

Since strain-rates near a shear band are typically of the order of 10^5/s and the rate constant b equals 10^4 s or so, $bI \gg 1$ and $(1 + bI)^m \simeq (bI)^m$ within and adjacent to a shear band. Eq. (10) is thus replaced by $s = k_0 g(bI)^m$.

In the inertial region, as pointed out above, we neglect the effect of heat conduction, i.e. the first term on the left-hand side of Eq. (8). Furthermore, we assume the following asymptotic form of the solution in this region.

$$\phi = f_1 r^a \tilde{\phi}(\psi), \tag{21}$$

$$s = f_2 r^c \tilde{s}(\psi), \tag{22}$$

$$g = f_3 r^d \tilde{g}(\psi), \tag{23}$$

$$I = f_4 r^e \tilde{\imath}(\psi), \tag{24}$$

$$p = f_5 r^h \tilde{p}(\psi). \tag{25}$$

Here ϕ, $\tilde{s}$, $\tilde{g}$, $\tilde{\imath}$ and $\tilde{p}$ are non-dimensional functions of ψ only, a, c, d, e and h are constants, and f_1, f_2, f_3, f_4 and f_5 are dimensional quantities. Substituting from Eqs. (21)–(25) into Eqs. (8)–(17) and (20), and requiring that the variable r drop out of each equation in the limit as $r \to 0$, leaving only coupled ordinary differential equations in ψ, it is necessary that

$$\phi = \Gamma r^{\frac{2m+1}{1+m}} \tilde{\phi}(\psi), \tag{26}$$

$$s = \rho U \Gamma r^{\frac{m}{1+m}} \tilde{s}(\psi), \tag{27}$$

$$g = \frac{\alpha}{c_v} \Gamma^2 \, r^{\frac{2m}{1+m}} \tilde{g}(\psi), \tag{28}$$

$$I = \Gamma r^{\frac{-1}{1+m}} \tilde{\imath}(\psi), \tag{29}$$

$$p = \rho U \frac{1+m}{m} \Gamma r^{\frac{m}{1+m}} \tilde{p}(\psi), \tag{30}$$

and that functions $\tilde{\phi}$, $\tilde{s}$, $\tilde{g}$, $\tilde{\imath}$ and $\tilde{p}$ satisfy

$$(\tilde{g} \tilde{\imath}^{m-1} \tilde{x}_1)'' + 4 \frac{2m^2 + m}{(1+m)^2} (\tilde{g} \tilde{\imath}^{m-1} \tilde{\phi}')' - \frac{3m^2 + 2m}{(1+m)^2} (\tilde{g} \tilde{\imath}^{m-1} \tilde{x}_1) = \tilde{x}''_2 + \frac{m^2}{(1+m)^2} \tilde{x}_2, \tag{31}$$

$$\tilde{s} \tilde{\imath} = \frac{2m}{1+m} \cos \psi \tilde{g} - \sin \psi \tilde{g}', \tag{32}$$

$$\tilde{s} = \tilde{g} \tilde{\imath}^m, \tag{33}$$

$$\tilde{\imath} = \left[\frac{4m^2}{(1+m)^2} (\tilde{\phi}')^2 + \tilde{x}_1^2 \right]^{1/2}, \tag{34}$$

$$\tilde{p} = (\tilde{g} \tilde{\imath}^{m-1} \tilde{x}_1)' + 2 \frac{3m^2 + 2m}{(1+m)^2} (\tilde{g} \tilde{\imath}^{m-1} \tilde{\phi}') - \tilde{x}'_2, \tag{35}$$

where

$$\Gamma = \left(\frac{\rho c_{\mathrm{v}} U}{\alpha \ k_0 b^m} \right)^{\frac{1}{1+m}},$$

(36)

$$\tilde{x}_1 = \tilde{\phi}'' + \frac{2m+1}{(1+m)^2} \tilde{\phi},$$

(37)

$$\tilde{x}_2 = \sin \psi \tilde{\phi}' - \frac{2m+1}{1+m} \cos \psi \tilde{\phi},$$

(38)

and a prime denotes differentiation with respect to ψ. One can verify that Eqs. (26)–(30) are dimensionally correct. Eqs. (31)–(34) are nonlinear and coupled fourth-order ordinary differential equation for $\tilde{\phi}$ and second-order ordinary differential equation for $\tilde{g}$. They determine the angular distribution of the inertial solution.

Chen and Batra [26] have determined asymptotic fields near a stationary crack tip in a rigid thermoviscoplastic body undergoing either antiplane shear or plane strain deformations. In each case they found the effective stress and the effective plastic strain rate to behave as $r^{-m/(1+m)}$ and $r^{-1/(1+m)}$, respectively, as $r \to 0$. Both inertia and heat conduction effects were considered, and g was assumed to have the form $g_0(t) + f_3(t)r^h\tilde{g}(\theta)$ near the crack tip. For the problem studied herein, the deformation fields appear steady to an observer situated on and moving with the shear band tip. The order of singularity in the two problems turns out to be same for the effective plastic strain rate but different for the effective stress. The order of singularity for s, g and I in the present shear band problem is the same as that found by Wright and Walter [19] for a shear band propagating at a uniform velocity in a rigid thermoviscoplastic body deformed in antiplane shear. They grouped the terms differently. Rewriting Eq. (28) as

$$g = \frac{\rho U^2}{k_0} \left(\frac{\rho c_{\mathrm{v}}}{\alpha k_0} \right)^{\frac{(1-m)}{(1+m)}} \left(\frac{r}{Ub} \right)^{\frac{2m}{1+m}} \tilde{g}(\psi)$$

we see that g varies as U^2 implying thereby that the temperature ahead of the shear band decreases sharply for faster propagation of the shear band. Eq. (30) implies that at a fixed value of r, the hydrostatic pressure in the inertial region increases rapidly as m approaches zero.

Henceforth, we set $t = 0$ in the present configuration so that $\bar{r} = r$ and $\psi = \theta$; this facilitates the interpretation of the results.

2.2. Boundary conditions for the inertial solution

For in-plane shear or mode II deformations, the radial velocity $u = (1/r)\phi_{,\theta}$ is an odd function of θ. Hence, ϕ is an even function of θ. Since the temperature is an even function of θ, therefore, $\tilde{g}$ is also an even function of θ. Hence

$$\tilde{\phi}'(0) = \tilde{\phi}'''(0) = \tilde{g}'(0) = 0.$$

(39)
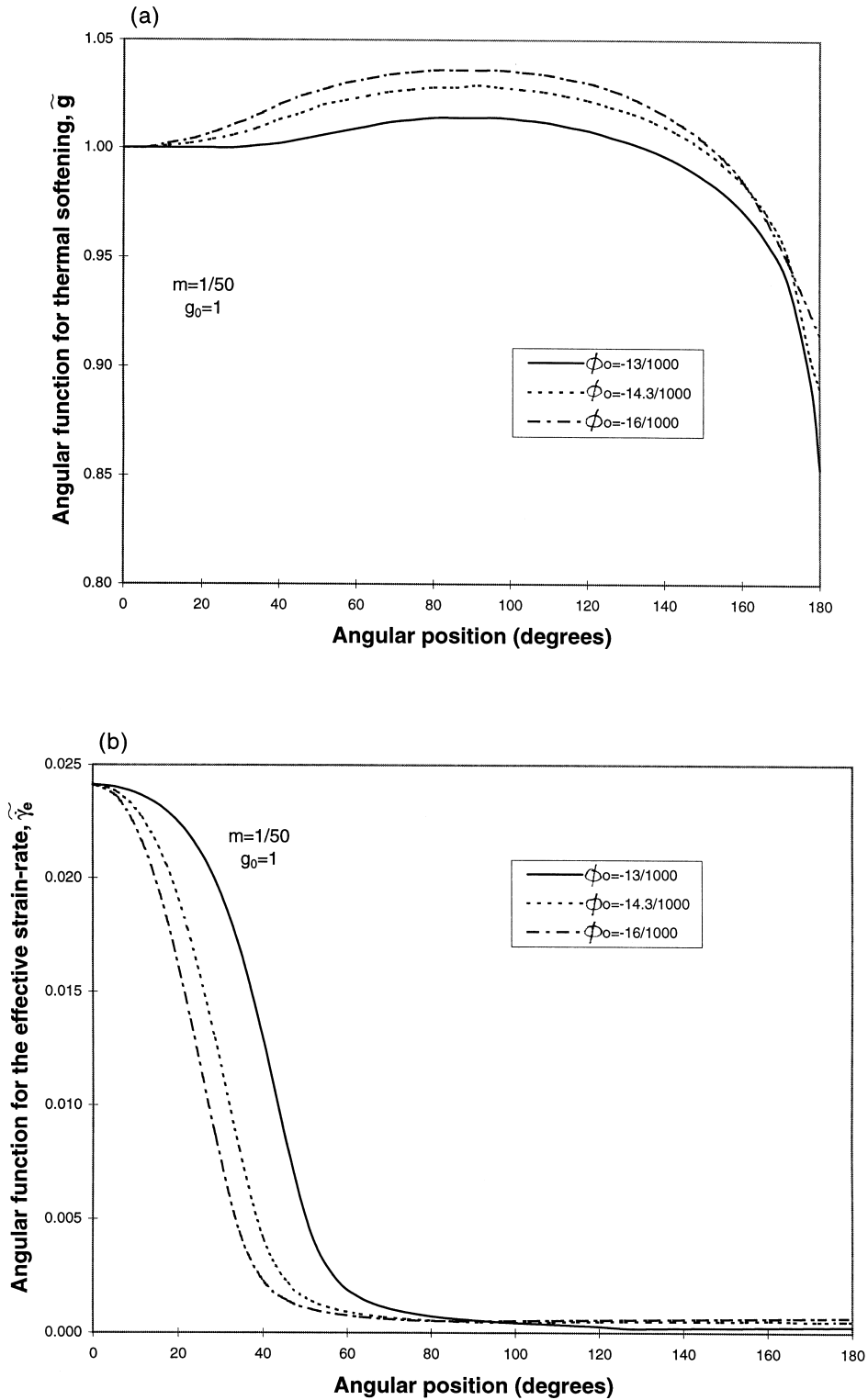
Fig. 2. Angular distribution of: (a) the thermal softening function $\tilde{g}$; (b) the effective plastic strain-rate; (c) the effective stress; and (d) the hoop stress for $\phi_0 = -0.013$, -0.0143 and -0.016, $g_0 = 1$, $m = 0.02$.

(c)

m=1/50
$g_0=1$

o=-13/1000
o=-14.3/1000
o=-16/1000

Angular function for the effective stress, $\tilde{\sigma}_e$

Angular position (degrees)

(d)

m=1/50
$g_0=1$

ϕ_o=-13/1000
ϕ_o=-14.3/1000
ϕ_o=-16/1000

Angular function for the hoop stress, $\tilde{\sigma}_{\theta\theta}$

Angular position (degrees)
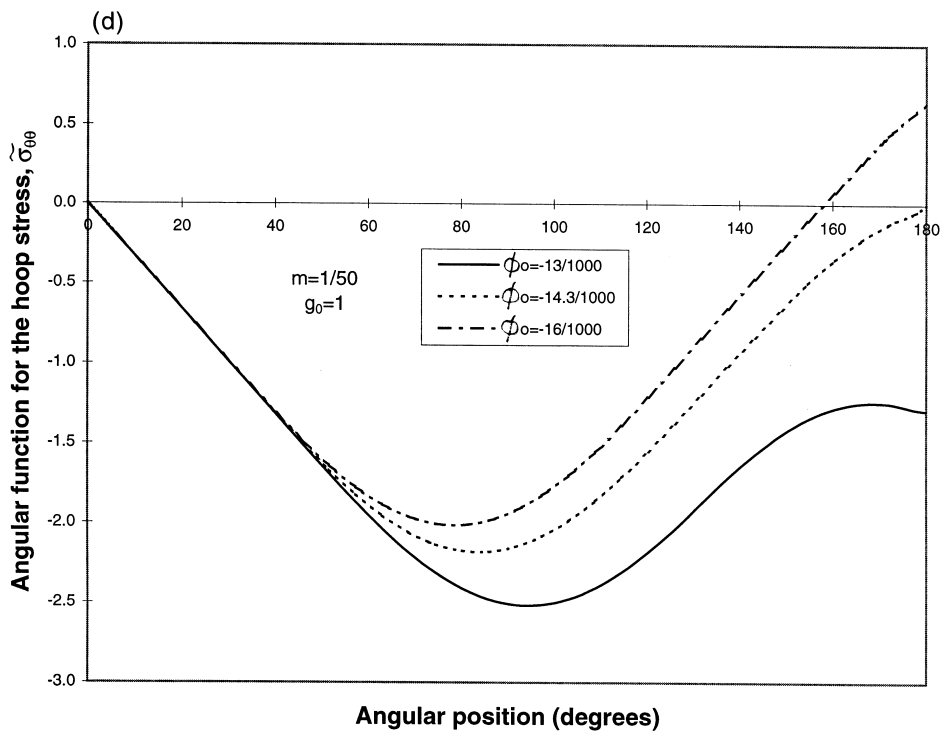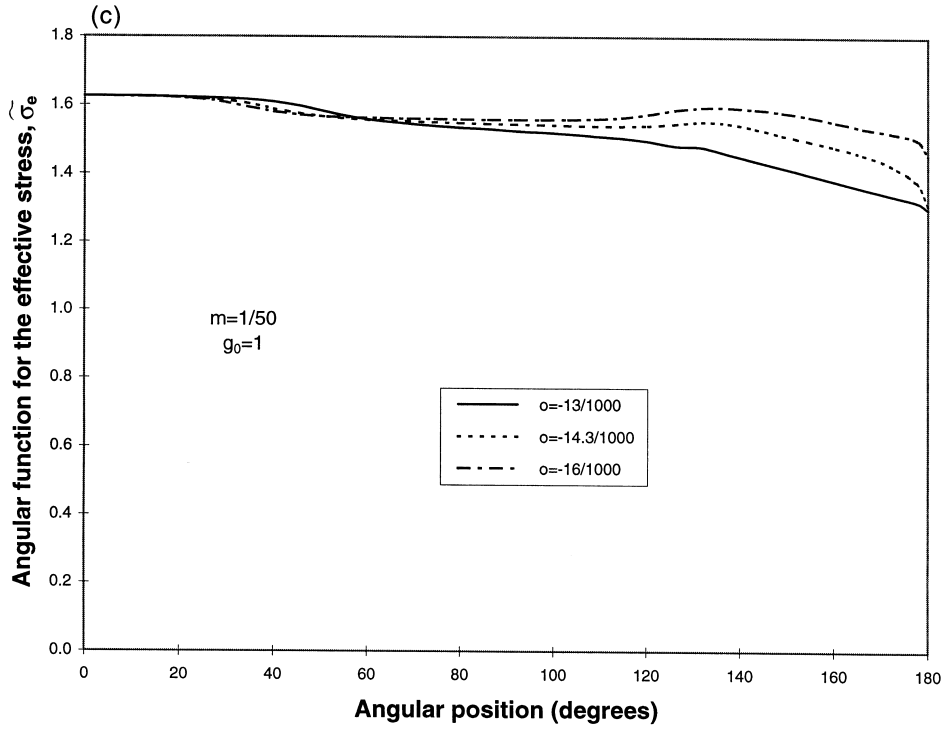
Fig 2 (*continued*)

Eqs. (32) and (33) yield

$$\tilde{g}' \sin \theta = \tilde{g}\left(\frac{2m}{1+m}\cos \theta - \tilde{\imath}^{m+1}\right). \tag{40}$$

Evaluating this equation at $\theta = 0$, assuming that $\tilde{g}(0) \neq 0$, recalling Eqs. (34), (37) and (39), we obtain

$$\tilde{\phi}''(0) = \left(\frac{2m}{1+m}\right)^{\frac{1}{1+m}} - \frac{2m+1}{(1+m)^2}\tilde{\phi}(0). \tag{41}$$

In order to solve Eqs. (31)–(35) for $\tilde{\phi}$ and $\tilde{g}$, we need six boundary conditions but Eqs. (39) and (41) constitute only four boundary conditions. A possibility is to regard $\tilde{g}(0)$ and $\tilde{\phi}(0)$ parameters and find solutions of Eqs. (31)–(35) for various values of $\tilde{g}(0)$ and $\tilde{\phi}(0)$. Numerical experiments show that solutions of Eqs. (31)–(35) for different values of $\tilde{g}(0) \equiv g_0$ are similar to each other, however, these equations have a solution only for values of *de*] > $\tilde{\phi}(0) \equiv \phi_0$ in a very narrow range; the solution technique is briefly discussed in the next section. Figs. 2(a)–(d) exhibit the variation of $\tilde{g}$, the effective stress $\tilde{\sigma}_e \equiv (\frac{3}{2}\text{tr}(SS^T))^{1/2}$, the effective plastic strain-rate $\tilde{\dot{\gamma}}_e \equiv (\frac{2}{3}\text{tr}(\tilde{D}\tilde{D}))^{1/2}$, and $\sigma_{\theta\theta}$ with θ for $g_0 = 1.0$, $m = 0.02$, and three different values of ϕ_0. It is clear that, for these three values of ϕ_0, results are qualitatively similar, and a higher value of $|\phi_0|$ results in a lower temperature rise and a higher value of the effective stress at $\theta \simeq 180°$. The angular width of the severely deforming region ahead of the shear band decreases with an increase in the value of $|\phi_0|$.

We can derive an additional boundary condition by exploiting the fact that an adiabatic shear band is usually very narrow, and only a few micrometers wide. Following Olmstead et al. [27], Wright and Walter [19] and Glimm et al. [28] we model it as a material singular surface. Equations expressing the balance of mass, linear momentum and internal energy across a material singular surface with no fluxes through its lateral edges and no production and supply of mass, linear momentum and internal energy in its interior, are (e.g. see Müller [29,30])

$$[\mathbf{v} \cdot \mathbf{n}] = 0, \tag{42}$$

$$[\boldsymbol{\sigma}\mathbf{n}] = 0, \tag{43}$$

$$[\mathbf{q} \cdot \mathbf{n}] + (\boldsymbol{\sigma}\mathbf{n}) \cdot [\mathbf{v}] = 0, \tag{44}$$

where $\mathbf{q} = -k\nabla T$ is the heat flux, $\mathbf{n}$ is a unit vector normal to the material singular surface, and $[f]$ denotes the jump of f across the material singular surface. Because heat conduction has been neglected in the inertial region, Eq. (44) will not be considered. For in-plane shear deformations, velocity $\mathbf{v}$ at $\theta = \pm\pi$ has components (u, v) and since $\mathbf{n} = (0, \pm1)$, and v is an even function of θ, therefore, Eq. (42) is identically satisfied. Eq. (43) requires that the tangential traction (shear stress) $\sigma_{r\theta}$ and the normal traction (hoop stress) $\sigma_{\theta\theta}$ at $\theta = \pm\pi$ be continuous across the material singular surface $\theta = \pm\pi$. Note that $\sigma_{r\theta}$ is an even function and $\sigma_{\theta\theta}$ is an odd function of θ. Therefore, the continuity of $\sigma_{\theta\theta}$ across the singular surface requires
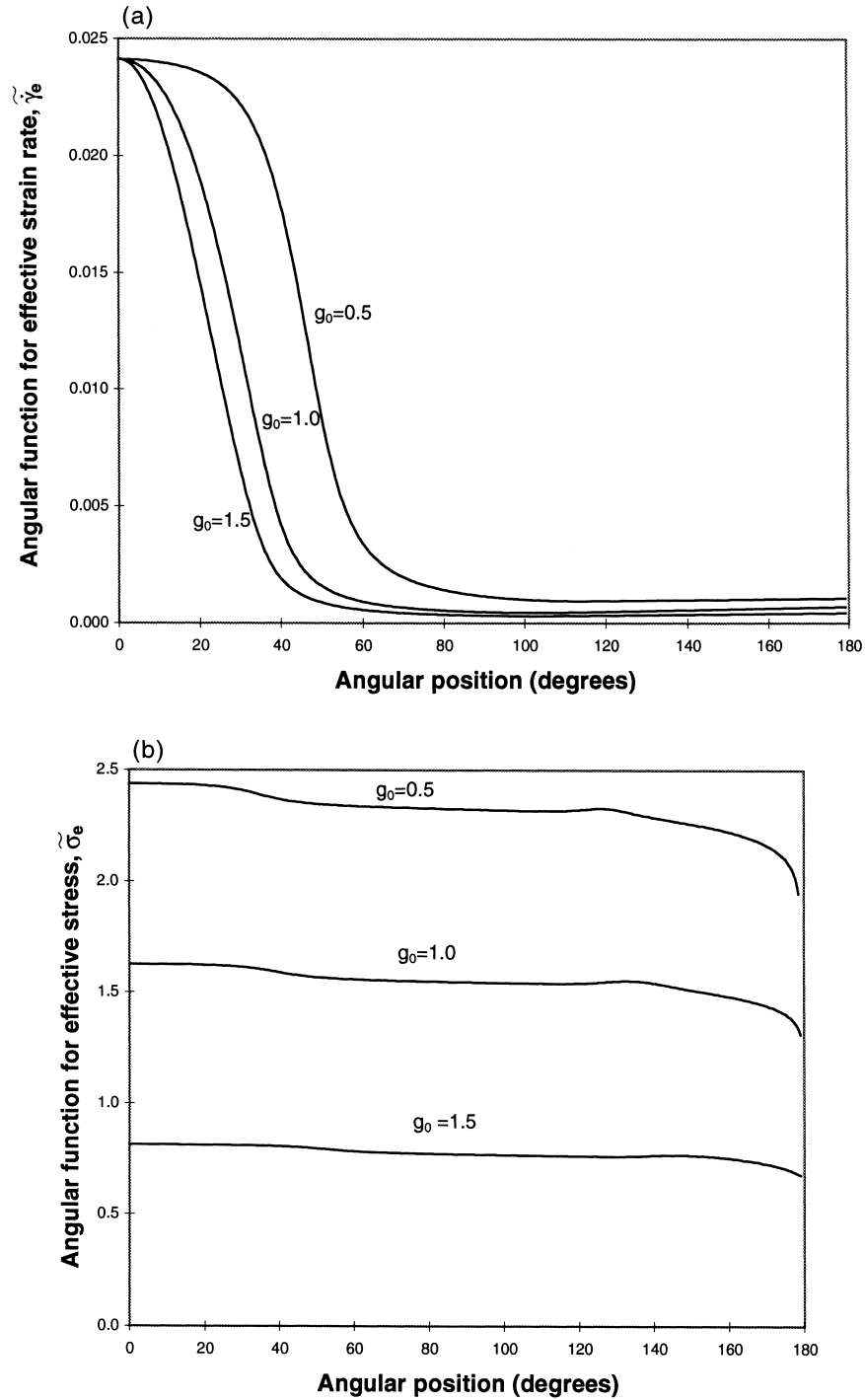
Fig. 3. Angular distribution of: (a) the effective plastic strain-rate; (b) the effective stress; (c) the thermal softening function; (d) the radial velocity; and (e) the circumferential velocity in the inertial region for $g_0 = 0.5$, 1.0, 1.5, and $m = 0.02$.
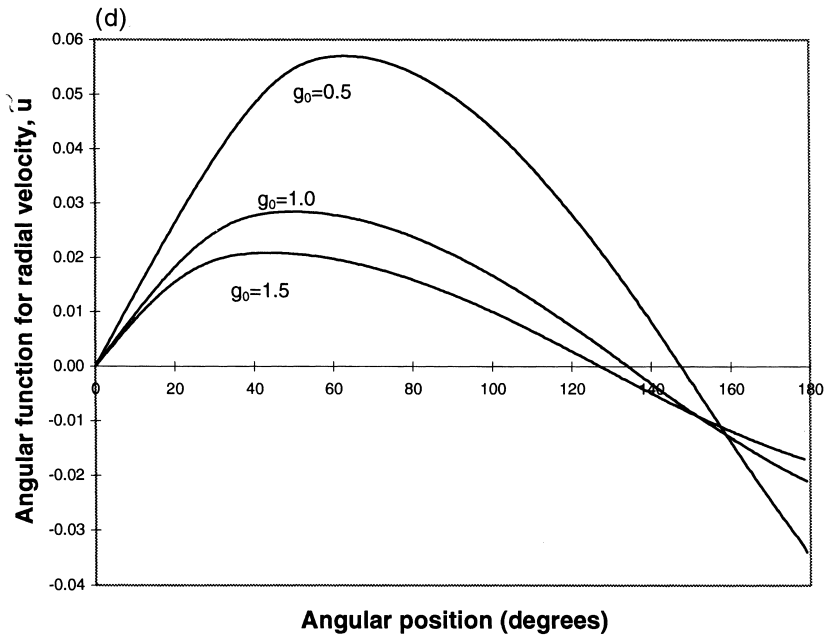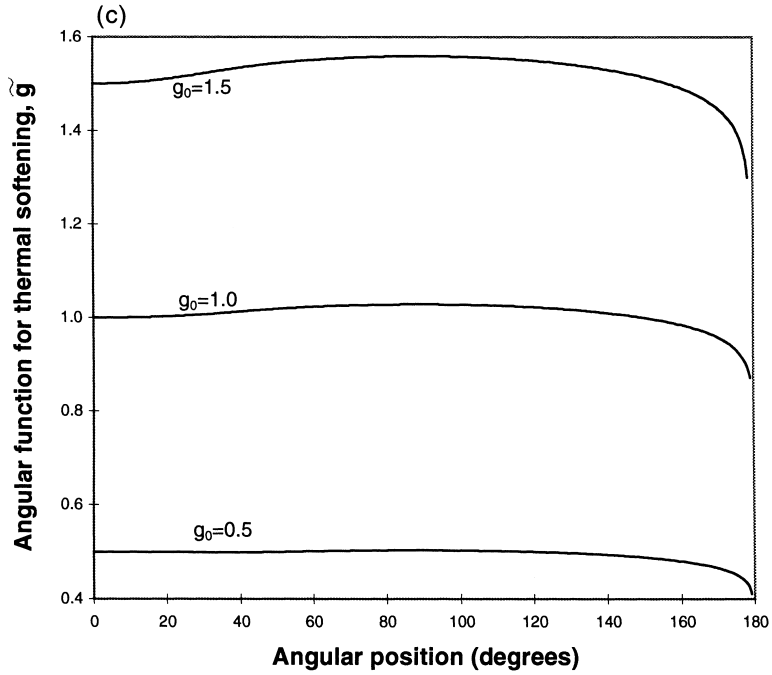
Fig. 3–(*continued*)
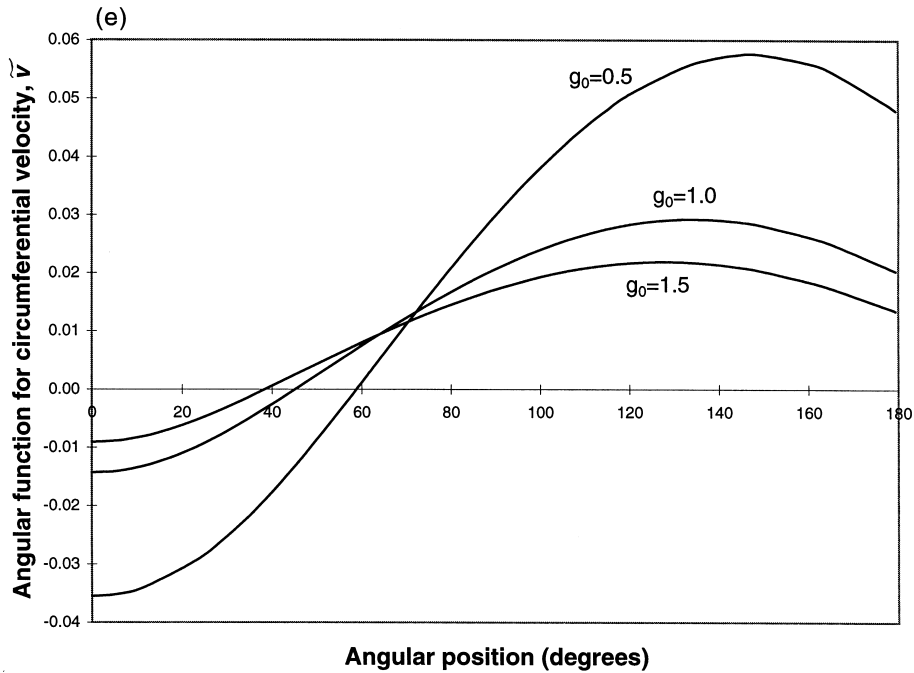
Fig. 3–(*continued*)

that $\sigma_{\theta\theta}|_{\theta=\pi^-} = 0$, or

$$\left(\frac{2m}{1+m} \tilde{g} \tilde{\imath}^{m-1} \tilde{\phi}' + \frac{1+m}{m} \tilde{p} \right)\Bigg|_{\theta=\pi^-} = 0. \tag{45}$$

We will comment in Section 3 on the discontinuity of the radial velocity and the continuity of shear tractions $\sigma_{r\theta}$ across the singular surface.

2.3. Numerical results

Coupled and nonlinear ordinary differential Eqs. (31) and (32) under five boundary conditions (39), (41) and (45) are solved over the interval $(0, \pi)$ by the fourth-order Runge–Kutta integration scheme and the shooting method. Let **A** be a six-dimensional vector with components $\tilde{\phi}$, $\tilde{\phi}'$, $\tilde{\phi}''$, $\tilde{\phi}'''$, $\tilde{g}$ and $\tilde{g}'$. Then, Eqs. (31) and (32) can be written as

$$\mathbf{A}' = \mathbf{f}(\mathbf{A}, \theta) \tag{46}$$

where a prime denotes differentiation with respect to θ. In order to solve Eq. (46) by the fourth-order Runge–Kutta method, $\mathbf{A}(0)$ needs to be prescribed. Here $\tilde{\phi}(0)$ and $\tilde{g}(0)$ are not known but Eq. (45) provides a relation among components of **A** evaluated at $\theta = \pi^-$. Note that $\tilde{p}$ given by Eq. (35) is determined by **A**. We regard $\tilde{g}(0) = g_0$ as a parameter (e.g. see Ref. [19]) and solve Eq. (46) for numerous values of $\tilde{\phi}(0)$ till the magnitude of the left-hand side of
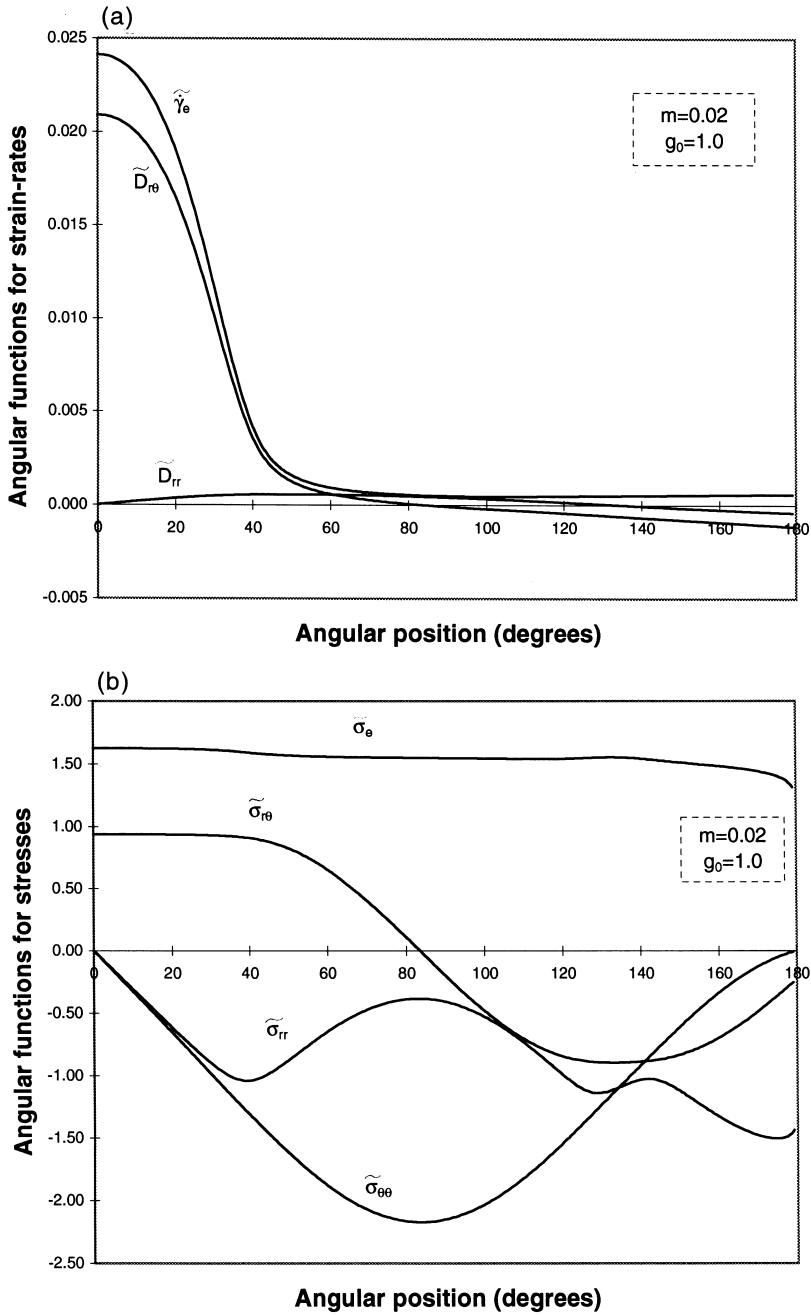
Fig. 4. Angular distribution of: (a) different components of the strain-rate tensor; and (b) different components of the stress tensor in the inertial region for $g_0 = 1.0$ and $m = 0.02$.
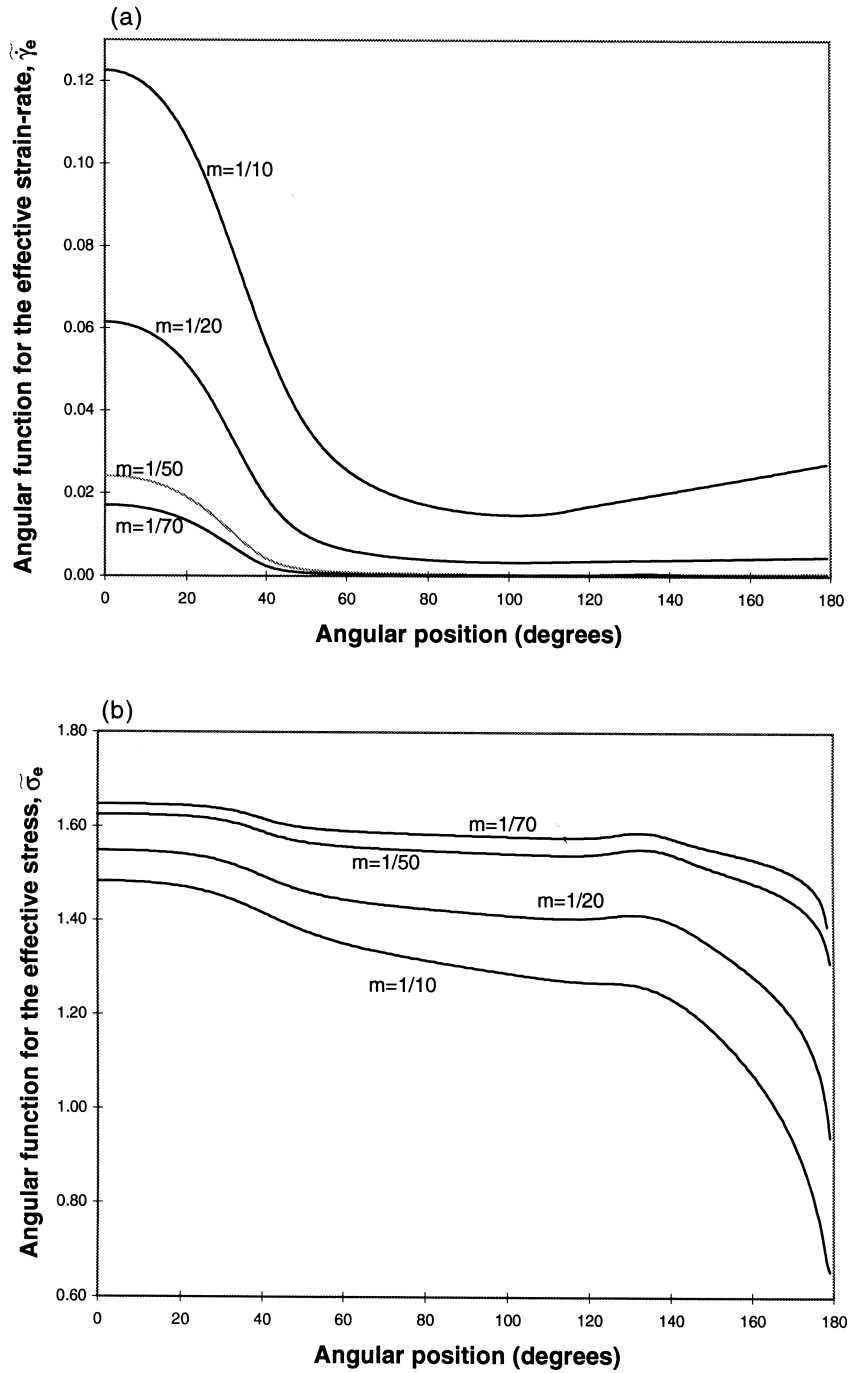
Fig. 5. Effect of the strain-rate sensitivity *m* upon the angular distribution of: (a) the effective plastic strain-rate; (b) the effective stress; (c) the thermal softening function; and (d) the radial velocity in the inertial region.
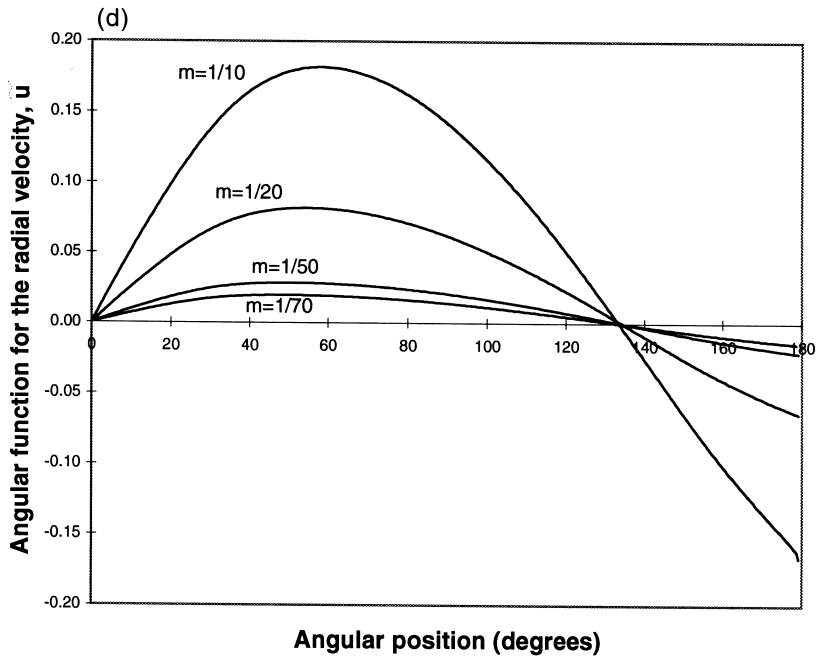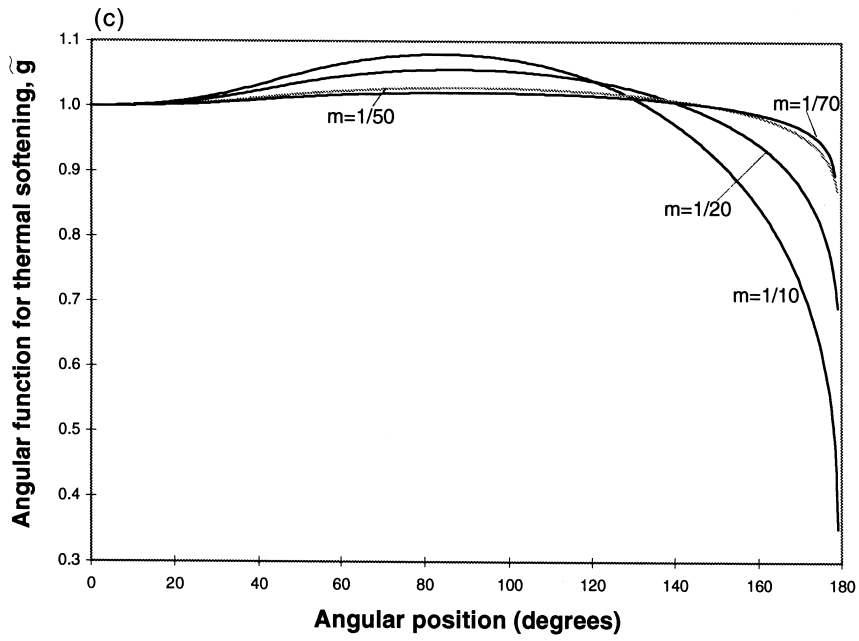
Fig 5 (*continued*)

Eq. (45) is less than 10^{-3}. Since the coefficient of $\tilde{g}'$ in Eq. (32) vanishes at $\psi = \theta = 0$, Eqs. (39) and (41) are assumed to hold at $\theta_0 = 10^{-5}$ and Eqs. (31)–(35) integrated over $(10^{-5}, \pi - 10^{-5})$. Numerical experiments with $\theta_0 = 10^{-6}$, 10^{-7} and 10^{-8} gave results identical with those obtained with $\theta_0 = 10^{-5}$.

Figs. 3(a)–(e) depict the variation vs θ of the angular functions for the effective plastic strain-rate, $\tilde{\dot{\gamma}}_e$, the effective stress, $\tilde{\sigma}_e$, the thermal softening function, $\tilde{g}$, the radial velocity $\tilde{u}$, and the circumferential velocity $\tilde{v}$ for $g_0 = 0.5$, 1.0 and 1.5 and the strain-rate sensitivity parameter $m = 0.02$. The only material parameter appearing in Eqs. (31) and (32) is the strain-rate sensitivity m, so the results presented in Fig. 3 are valid for all thermoviscoplastic materials obeying the constitutive relation (4). These results indicate that the basic behavior of the inertial solution is not affected by the value of g_0. In torsional tests on thin-walled 4340 steel tubes, Marchand and Duffy [4] estimated the speed of a shear band to be either 260 m/s or 520 m/s according to the way the band propagated circumferentially, either in one direction or simultaneously in both directions. Batra and Zhang [31] numerically simulated Marchand and Duffy's test and found that a shear band originating from a point propagated simultaneously in both directions at the same speed. Their computations also show that the shear band speed strongly depends upon the nominal strain-rate. At a nominal strain-rate of 5000/s, the shear band speed was found to increase from 180 m/s at the point of initiation to 1080 m/s when the shear band reached the diametrically opposite end. For the material parameters listed earlier for a typical hard steel and $U = 200$ m/s, an increment of -0.1 in g_0 corresponds to an increment in T of about 56.6 K at $r = 10$ μm. Thus a large temperature rise near the shear band tip does not influence the basic behavior of the inertial solution. These plots also indicate that straight ahead of the propagating shear band, i.e. $\theta = 0$, the effective stress and the effective plastic strain-rate are maximum, but the maximum temperature rise, $T = (1 - g)/\alpha$, occurs at $\theta = \pi^-$.

Plots in Fig. 3(a) of the effective plastic strain-rate vs θ suggest that for $g_0 = 0.5$ only the material ahead of the shear band lying in the arc $-60° \leqslant \theta \leqslant 60°$ is severely deformed; this sector becomes narrower as the value of g_0 increases or the temperature decreases. The effective stress remains essentially unchanged in this sector [cf. Fig. 3(b)]. The temperature is a little bit higher straight ahead of the band and is highest at points close to $\theta \simeq 180°$. As the temperature at $\theta = 0°$ increases or g_0 decreases, the angular position of the point where the maximum radial velocity occurs changes from $\theta \simeq 40°$ to $\theta \simeq 60°$. The circumferential velocity is negative at $\theta = 0$ and positive at $\theta \simeq \pi$, suggesting, thereby, a wavy shear band surface.

Fig. 4(a) depicts the plot of the angular function for D_{rr}, $D_{r\theta}$ and $\dot{\gamma}_e$ vs θ for $g_0 = 1.0$ and $m = 0.02$. It is evident that the normal strain rate $D_{rr}(= -D_{\theta\theta})$ contributes very little to the effective plastic strain-rate and the shear strain-rate $D_{r\theta}$ assumes significant values in the sector $-40° < \theta < 40°$. From the plot of the angular function for the stresses in Fig. 4(b), we see that straight ahead of the shear band, the normal stresses σ_{rr} and $\sigma_{\theta\theta}$ vanish and the shear stress $\sigma_{r\theta}$ is maximum. The boundary condition (45) requires that $\sigma_{\theta\theta}$ vanish at $\theta \simeq 180°$. Figs. 5(a)–(d) exhibit the effect of the strain-rate sensitivity parameter m upon the angular functions for the effective plastic strain-rate, effective stress, thermal softening function g and the radial velocity. The general nature of the angular distribution of these functions is unaffected by the value of m.

3. Core solution

As suggested by Wright and Walter [19], the one-dimensional theory of adiabatic shear bands is assumed to be adequate in the core region behind the shear band tip. For small values of the strain-rate sensitivity parameter m, Glimm et al. [28] have derived the asymptotic expressions for the temperature and velocity distributions near the band center. Wright and Walter [19] and Wright and Ockendon [32] have derived Eqs. (48) and (49) below for an affine thermal softening function.

$$T = T_c - \frac{2mg(T_c)}{\alpha}\ln\left[\cosh\left(\frac{y}{\delta}\right)\right][1 + O(m)], \tag{47}$$

$$g(T_c) = \left(\frac{1}{k_0 b^m}\right)^{\frac{1}{1-m}}\left(\frac{2km}{\alpha}\right)^{\frac{m}{1-m}}|\tau|\left(\frac{1}{2}|\Delta V|\right)^{\frac{-2m}{1-m}}, \tag{48}$$
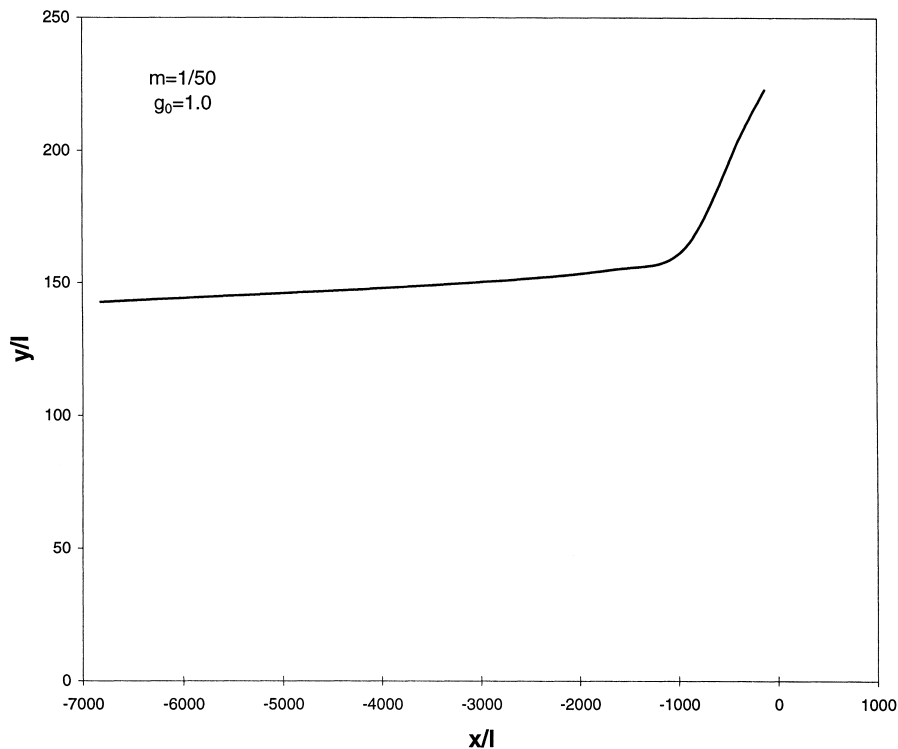
Fig. 6. Variation of half of the thermal width of the band behind the shear band tip.

$$\delta = \left(\frac{2km}{\alpha \left(\frac{1}{2} \mid \Delta V \mid \right)^{1+m} k_0 b^m} \right)^{\frac{1}{1-m}}. \tag{49}$$

Here T_c is the temperature rise at the band center, δ a measure of the shear band width, τ is the magnitude of the shear stress which is assumed to be constant within the band, $\mid \Delta V \mid$ is the magnitude of the jump in the velocity across the band, and y is the y-coordinate of a point in the rectangular Cartesian coordinate system attached to the shear band tip (cf. Fig. 1). The shear band is assumed to have finite width, which is inconsistent with the earlier assumption that it is a singular surface. For a nonzero but minuscule width of the shear band, the jump in the radial velocity can be related to the stress and temperature within the band through the constitutive relation (4) (for example, see Eq. (47) of Ref. [28]). Thus, the strain-rate within the band is very large but finite, and as the band width shrinks to zero, the strain-rate within the band approaches a Dirac-delta function.

In the mode-II deformations studied herein, the radial velocity $u = (1/r)\phi_{,\theta}$ and the tangential velocity $v = -\phi_{,r}$ are odd and even functions of θ, respectively. Using Eqs. (12)–(16) and (26)–(30) behind the band tip, we have

$$\tau = \sigma_{xy} = [\sigma_{r\theta}(\cos^2 \theta - \sin^2 \theta) - (\sigma_{\theta\theta} - \sigma_{rr})\sin \theta \cos \theta]|_{r=R_b},$$
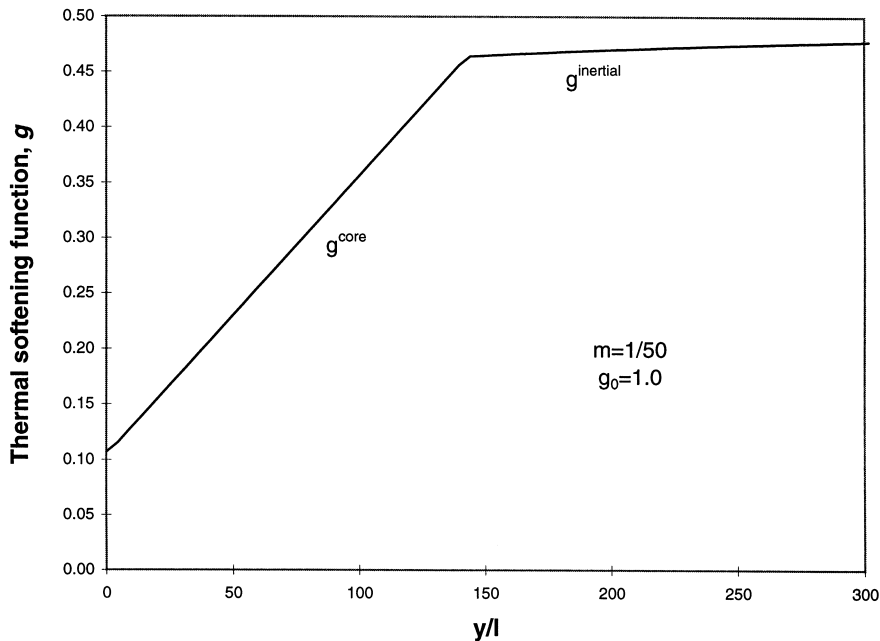
Fig. 7. Variation of the thermal softening function along $\theta \simeq \pi$ direction in core and inertial regions.

$$= \rho U \Gamma r^{\frac{m}{1+m}} \left[\tilde{g} \tilde{i}^{m-1} \tilde{x}_1 (\cos^2 \theta - \sin^2 \theta) + \frac{4m}{1+m} \tilde{g} \tilde{i}^{m-1} \tilde{\phi}' \sin \theta \cos \theta \right] \Bigg|_{r=R_b}, \tag{50}$$

$$\Delta V = u_x^+ \big|_{r=R_b} - u_x^- \big|_{r=R_b} = (u \cos \theta - v \sin \theta)^+ \big|_{r=R_b} - (u \cos \theta - v \sin \theta)^- \big|_{r=R_b},$$

$$= 2\Gamma r^{\frac{m}{1+m}} \left(\tilde{\phi}' \cos \theta + \frac{1+2m}{1+m} \tilde{\phi} \sin \theta \right) \Bigg|_{r=R_b}, \tag{51}$$

where u_x is the component of the velocity along the x-axis, and $2R_b \sin \theta$ may be thought of as the thermal width of the shear band.

Eqs. (11) and (47) imply that

$$g(y) = g(T_c)[1 + 2m \ln(\cosh(y/\delta))] \tag{52}$$

in the core region behind the band tip. Eq. (28) gives the distribution of the thermal softening function in the inertial region. Requiring that behind the band tip, the temperature from the core region equals that for the inertial region at the core/inertial region interface, we obtain

$$\frac{\alpha}{c_v} \Gamma^2 R_b^{\frac{2m}{1+m}} \tilde{g}(\theta) = g(T_c) \left[1 + 2m \ln \left(\cosh \frac{R_b}{\delta} \sin \theta \right) \right], \tag{53}$$
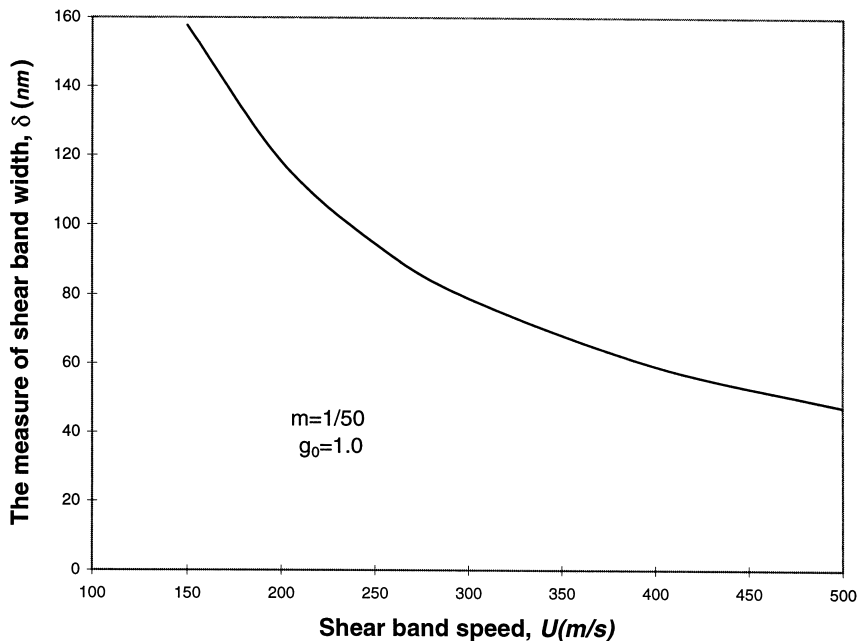
Fig. 8. Dependence of the measure of shear band width upon the shear band speed.
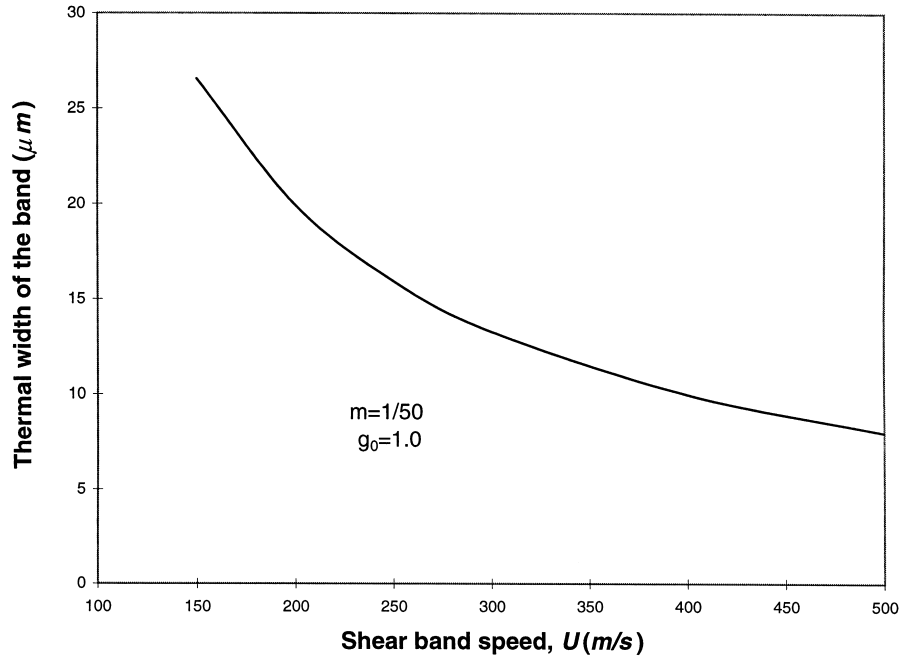
Fig. 9. Dependence of the thermal width of the band upon the shear band speed.
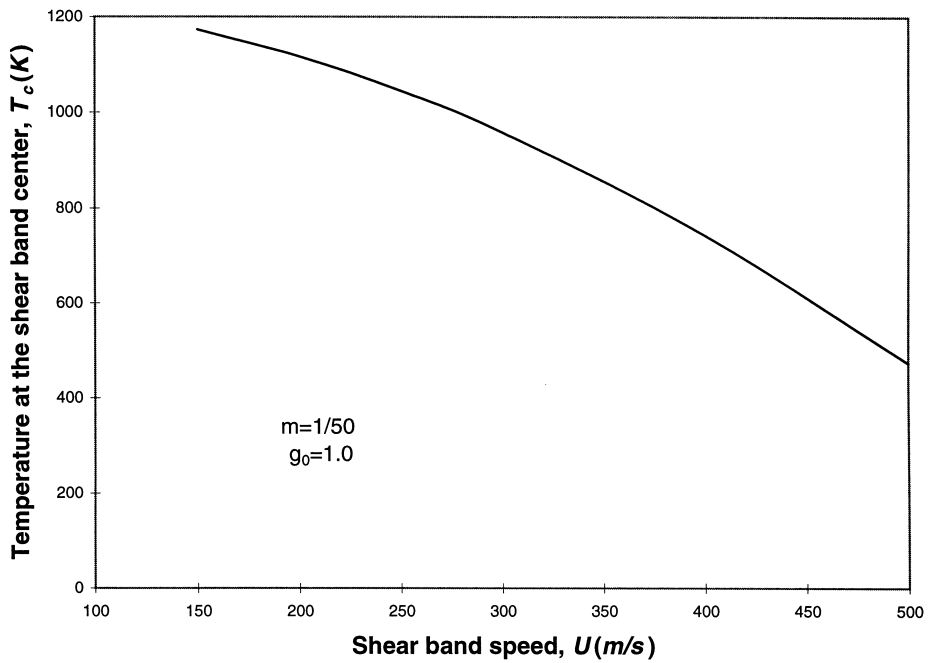
Fig. 10. Dependence of the temperature rise at the shear band center upon the shear band speed.
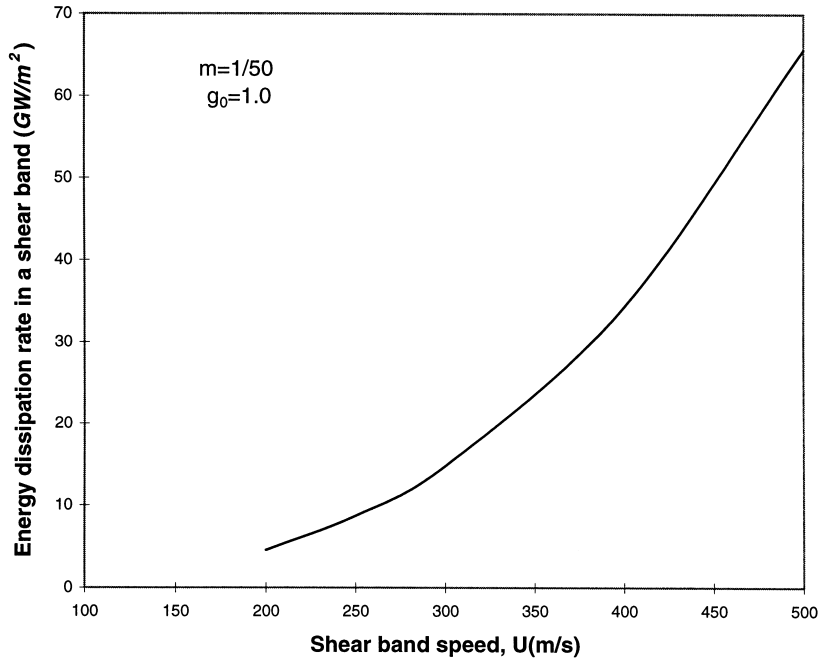
Fig. 11. Energy dissipation rate per unit surface area of the shear band at $\theta \simeq 180°$ vs the shear band speed.
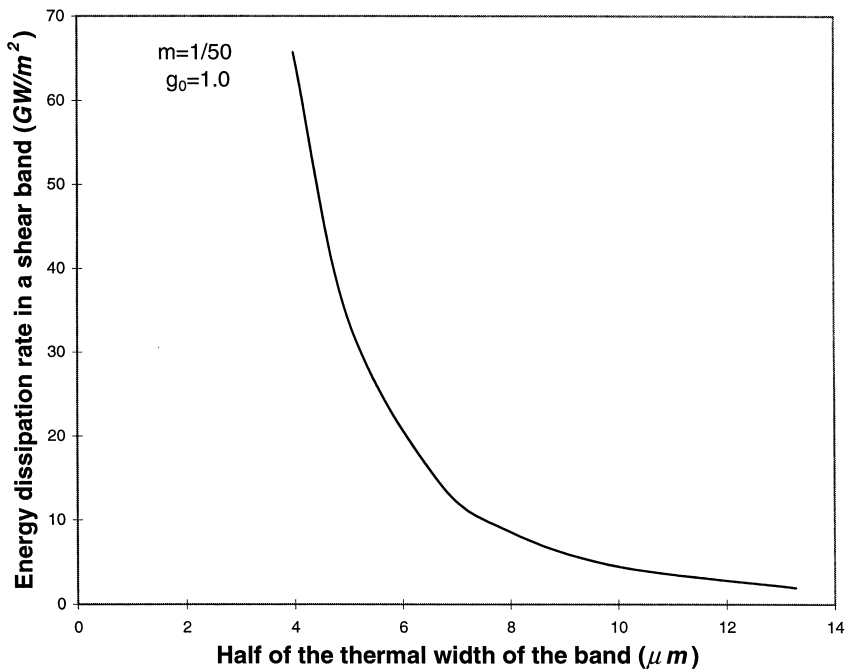
Fig. 12. Energy dissipation rate per unit surface area of the shear band vs the thermal width of the band at $\theta \simeq 180°$.

which determines R_b as a function of θ. Substitution from Eqs. (50) and (51) into Eqs. (47)–(49) and (52) yields T_c, $g(y)$ and δ. Fig. 6 shows the variation of half of the thermal width of the band with the distance from the band tip for $g_0 = 1.0$ where $l = k/(\rho c U) = 70$ nm. Thus, the width of the core region varies from about 32 µm very near the band tip to approximately 22 µm at a distance of about 350 µm behind the tip.

Fig. 7 depicts the variation of the thermal softening function in the core and inertial regions at $\theta \simeq 180°$ for the typical hard steel considered above with $g_0 = 1.0$. As expected, the temperature drops rapidly as one moves away from the center of the shear band. However, in the inertial region, because of the assumption of locally adiabatic deformations, the temperature rise decreases slowly. If we had solved the complete set of equations in the core region, then the temperature fields in the two regions would have blended smoothly rather than abruptly.

Figs. 8–10 exhibit the dependence of the measure δ of the shear band width, thermal width of the band at $\theta \simeq 180°$, and the temperature at the band center upon the shear band speed U for $g_0 = 1.0$. These results evince that δ, thermal width and the temperature rise at the shear band center decrease with an increase in the shear band speed, U. We note that for $U = 150$ m/s, thermal width $\simeq 27$ µm, and the observed widths of shear bands are close to 20 µm.

As noted above, the shear stress is taken to be constant within the shear band. Thus the rate of energy dissipated in the band equals the working of the shear tractions. Since the tangential force acting on a unit surface area of the shear band equals τ, the working of the surface traction will equal $\tau(\Delta V)$. Grady [33] has identified this working of surface tractions as the rate of energy dissipated within the band. Thus, the energy dissipated per second per unit surface area of the shear band equals $\tau \Delta V$ and, is a function of the angular position θ. For $\theta \simeq 180°$, and the typical hard steel, it is plotted in Fig. 11 as a function of the shear band speed. It is clear that the rate of energy dissipated per unit surface area of the shear band increases rapidly with an increase in the shear band speed. Fig. 12 exhibits this energy dissipation rate as a function of the thermal width of the band at $\theta \simeq 180°$. The energy dissipation rate drops drastically with an increase in the thermal width; this is consistent with Grady's [33] results.

4. Conclusions

We have determined an asymptotic solution near the shear band tip of equations governing thermomechanical deformations of a rigid thermoviscoplastic body deformed in mode II. It is assumed that deformations appear steady to an observer always situated on the shear band tip which moves with a uniform speed U. The region around the shear band front is divided into two parts—the core region behind the shear band tip and the inertial region excluding the core region and a small region around the shear band tip. In the inertial region, the inertia effects play a dominant role but heat conduction is neglected, and, in the core region, both inertia and heat conduction effects are important. The thermal width of the band as a function of the angular position θ is determined by ensuring that the temperature is continuous across the interface between the core and inertial regions. The asymptotic solution in the inertial region is found in terms of two parameters—the shear band speed and the value of the thermal softening function just ahead of the shear band tip. The structure of the asymptotic solution

predominantly depends only upon the material strain-rate sensitivity m; other material parameters and the shear band speed enter through the combination illustrated in Eq. (36). The nature of the asymptotic solution is essentially unaffected by the value assigned to the thermal softening function at $\theta = 0$. In the core region, the temperature gradient is high. The measure of the shear band width, the thermal width of the band at $\theta \simeq 180°$ and the temperature rise at the band center decrease with an increase in the speed U of the shear band; the first two seem to approach non-zero limiting values. For a typical hard steel and shear band speed equal to 200 m/s the measure of the shear band width equals about 100 nm and the thermal width of the band at $\theta \simeq 180°$ approximately 20 μm. Since observed shear bands are usually a few micrometers wide, it appears that the thermal width of the band at $\theta \simeq 180°$ is a good measure of the shear band width. At $U = 200$ m/s, the energy dissipation rate within the shear band equals approximately 5 GW per square meter of the surface area of the shear band and increases sharply with an increase in the band speed.

Acknowledgements

References

[1] H. Tresca, On further application of the flow of solids, Proc. Inst. Mech. Engr. 30 (1878) 301–345.

[2] H.F. Massey, The flow of metal during forging, Proc. Manchester Assoc. Engrs (1921) 21–26.

[3] C. Zener, J.H. Hollomon, Effect of strain rate on plastic flow of steel, J. Appl. Phys. 14 (1944) 22–32.

[4] A. Marchand, J. Duffy, An experimental study of the formation process of adiabatic shear bands in a structural steel 36 (1988) J. Mech. Phys. Solids, 251–283.

[5] R.C. Batra, C.H. Kim, Analysis of shear bands in twelve materials, Int. J. Plasticity 8 (1992) 75–89.

[6] B. Deltort, Experimental and numerical aspects of adiabatic shear in a 4340 steel, J. Physique, Colloque C8 4 (1994) 447–452.

[7] Y. Bai, B. Dodd, Adiabatic shear localization Occurrence, Theories and Applications, Pergamon Press, 1992.

[8] Y. Tomita, Simulations of plastic instabilities in solid mechanics, Appl. Mechs. Reviews 47 (1994) 171–205.

[9] H.M. Zbib, T. Shawki, R.C. Batra (Eds.), Material instabilities (special issue), Special Issue of Applied Mechanics Reviews 45 (1992) 3.

[10] R. Armstrong, R.C. Batra, M.A. Meyers, T.W. Wright (Eds.), Special issue on shear instabilities and viscoplasticity theories (special issue), Mech. Mater. 17 (1994) 485–498.

[11] P. Perzyna (Ed.), Localization and fracture phenomenon in inelastic solids, Springer, Berlin, 1998.

[12] R.C. Batra, D. Rattazzi, Adiabatic shear banding in a thick-walled steel tube, Comp. Mechs 20 (1997) 423–438.

[13] J.F. Kalthoff, Transition in the failure behavior of dynamically shear loaded cracks, Appl. Mech. Rev. 43 (1990) S247.

[14] J.J. Mason, A.J. Rosakis, G. Ravichandran, Full field measurements of the dynamic deformation field around a growing adiabatic shear band at the tip of a dynamically loaded crack or notch, J. Mech. Phys. Solids 42 (1994) 1679.

[15] M. Zhou, A.J. Rosakis, G. Ravichandran, Dynamically propagating shear bands in impact-loaded prenotched

plates—I. Experimental investigations of temperature signatures and propagation speed, J. Mech. Phys. Solids 44 (1996) 981.

[16] A. Needleman, V. Tvergaard, Analysis of brittle-ductile transition under dynamic shear loading, Int. J. Solids Structures 44 (1995) 2571–2590.

[17] M. Zhou, G. Ravichandran, A.J. Rosakis, Dynamically propagating shear bands in impact-loaded prenotched plates—II. Numerical simulations, J. Mech. Phys. Solids 44 (1996) 1007.

[18] R.C. Batra, N.V. Nechitailo, Analysis of failure modes in impulsively loaded prenotched steel plates, Int. J. Plasticity 13 (1997) 291.

[19] T.W. Wright, J.W. Walter, The asymptotic structure of an adiabatic shear band in antiplane motion, J. Mech. Phys. Solids 44 (1) (1996) 77–97.

[20] R.C. Batra, Steady state penetration of thermoviscoplastic targets, Comp. Mech. 3 (1988) 1–12.

[21] J. Litonski, Plastic flow of a tube under adiabatic torsion, Bull. Acad. Polonaise Sci. 25 (1977) 7–17.

[22] R.C. Batra, Pei-Rong Lin, Steady state axisymmetric deformations of a thermoviscoplastic rod striking a rigid cavity, Int. J. Impact Engng 8 (1989) 99–113.

[23] R.C. Batra, T. Gobinath, Steady state axisymmetric deformations of a thermoviscoplastic rod striking a thick thermoviscoplastic target, Int. J. Impact Engng 11 (1991) 1–31.

[24] R.C. Batra, De-Shin Liu, Adiabatic shear banding in plane strain problems, J. Appl. Mechs 56 (1989) 527–534.

[25] T.W. Wright, R.C. Batra, The initiation and growth of adiabatic shear bands, Int. J. Plasticity 1 (1985) 205–212.

[26] L. Chen, R.C. Batra, Shear instability direction at a crack tip in a thermoviscoplastic body, Theoretical & Appl. Fract. Mechs 29 (1998) 33–40.

[27] W.E. Olmstead, S. Nemat-Nasser, L. Ni, Shear band as surfaces of discontinuity, J. Mech. Phys. Solids 42 (1994) 697–709.

[28] J.G. Glimm, B.J. Plohr, D.H. Sharp, A conservative formulation for large deformation plasticity, Appl. Mech. Rev. 46 (1993) 519–526.

[29] I. Müller, Thermodynamics, Pittman, Boston, 1985.

[30] I. Müller, Thermodynamics of irreversible processes, Lecture Notes, Johns Hopkins Univ, Baltimore, 1971.

[31] R.C. Batra, X. Zhang, On the propagation of a shear band in a steel tube, J. Engng Mater. Technol. 116 (1994) 155–161.

[32] T.W. Wright, H. Ockendon, A model for fully formed shear bands, J. Mech. Phys. Solids 40 (1992) 1217–1226.

[33] D.E. Grady, Properties of an adiabatic shear-band process zone, J. Mech. Phys. Solids 40 (1992) 1197–1215.